

Figure S1. (a) Schematic of the experimental setup for conventional TiO₂ sintering. (b) The plot of temperature and time for the conventional sintering process. (c) The photo of conventional sintered TiO₂. (d) Schematic showing the experimental setup for flash sintering. (e) The plot of temperature, electric field, and current density during flash sintering. (f) The photo of flash sintered TiO₂ sample.

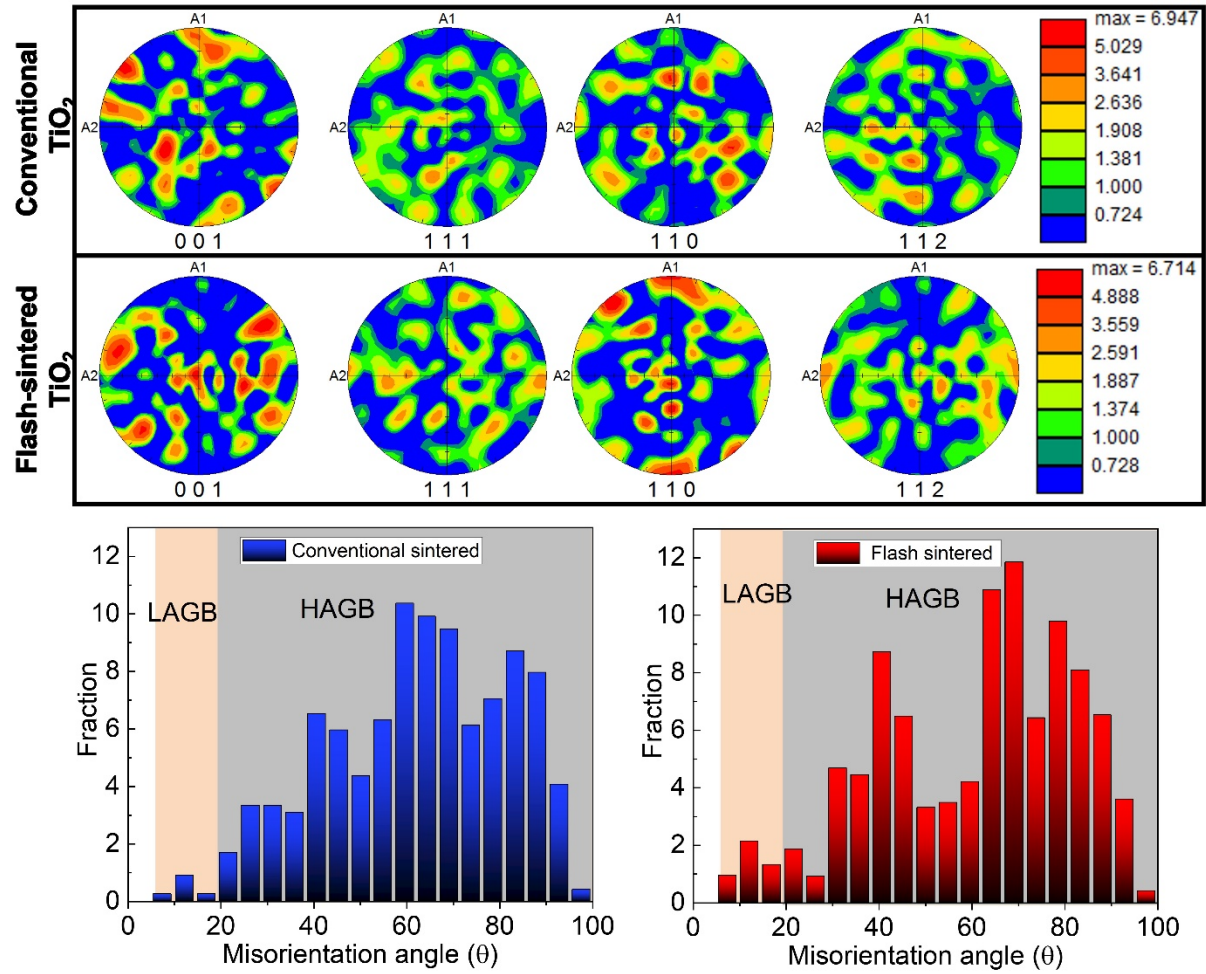


Figure S2. Texture and grain boundary distributions for the conventional and flash sintered TiO_2 specimens.

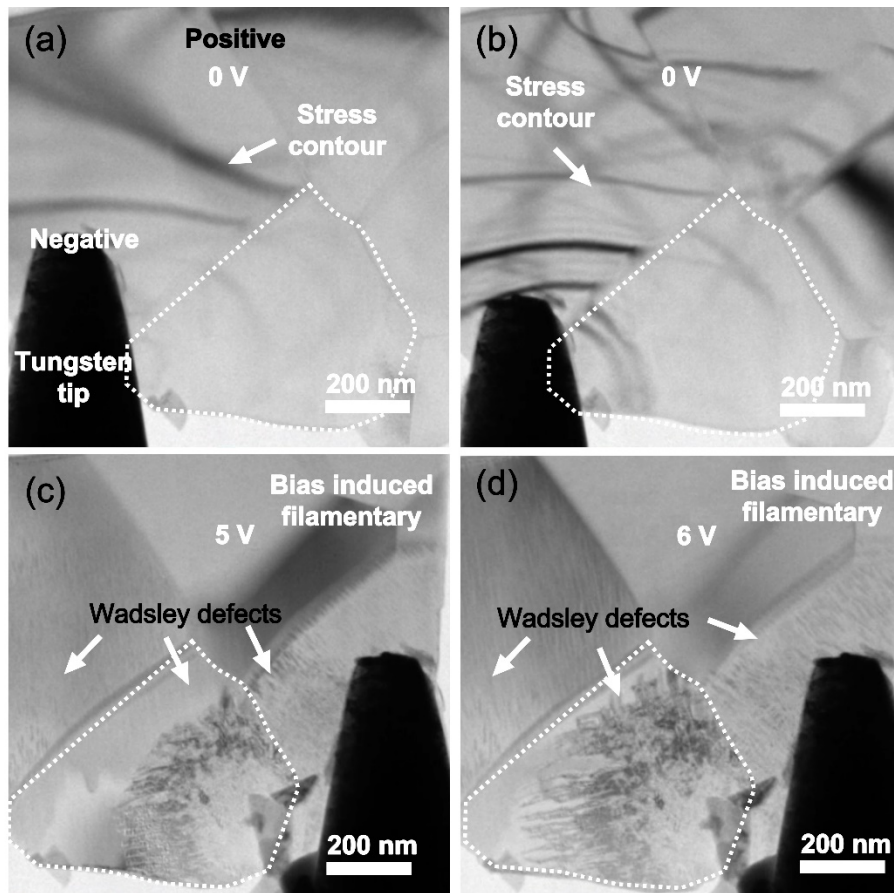


Figure S3. (a,b) TEM snapshots showing the stress contour migration triggered by movement of tip. (c,d) The defects propagation under electric bias.

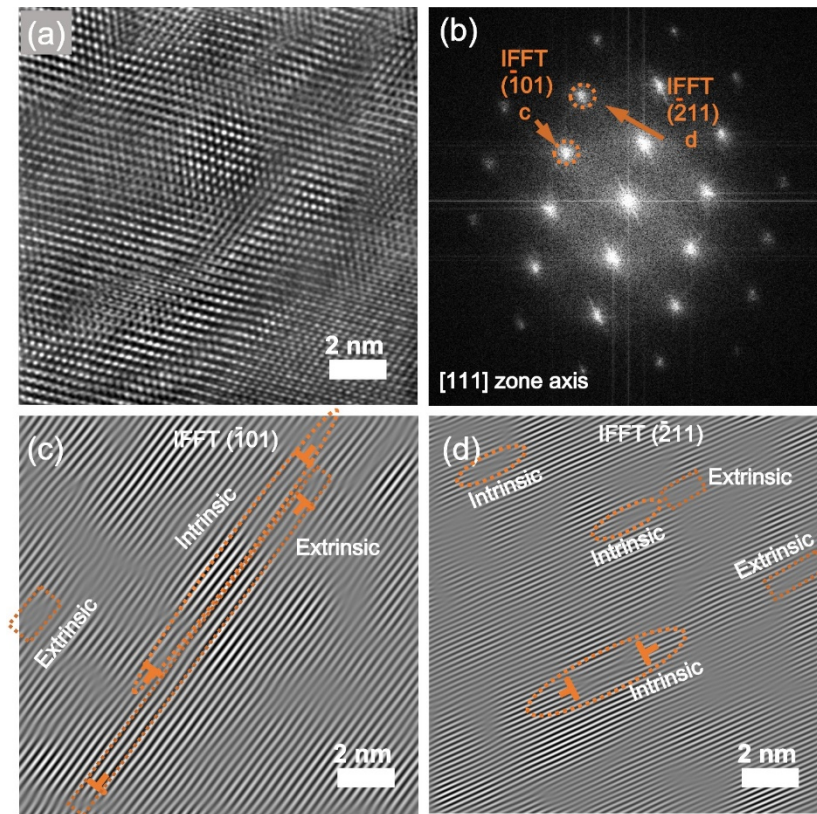


Figure S4. Postmortem HRTEM micrograph of the flash sintered TiO₂ sample showing the extrinsic and intrinsic nature of planar defects. (a) HRTEM micrograph of Wadsley defects formed under bias. (b) The FFT image of Fig. S3a. (c, d) IFFT images show the extrinsic and intrinsic planar defects along $(\bar{1}01)$ and $(\bar{2}11)$.

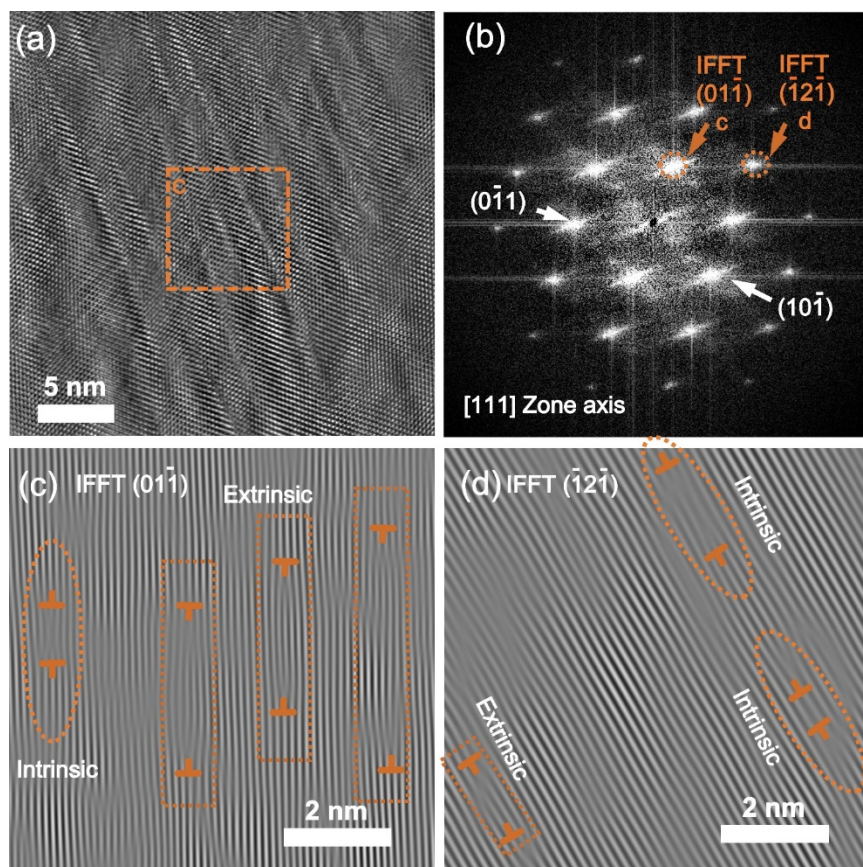


Figure S5. Postmortem HRTEM micrograph of the conventional sintered TiO_2 sample showing the extrinsic and intrinsic nature of planar defects. (a) HRTEM micrograph of Wadsley defects formed under bias. (b) The FFT image of area c in Fig. S4a. (c, d) IFFT images show the extrinsic and intrinsic planar defects along (011) and ($\bar{1}2\bar{1}$).

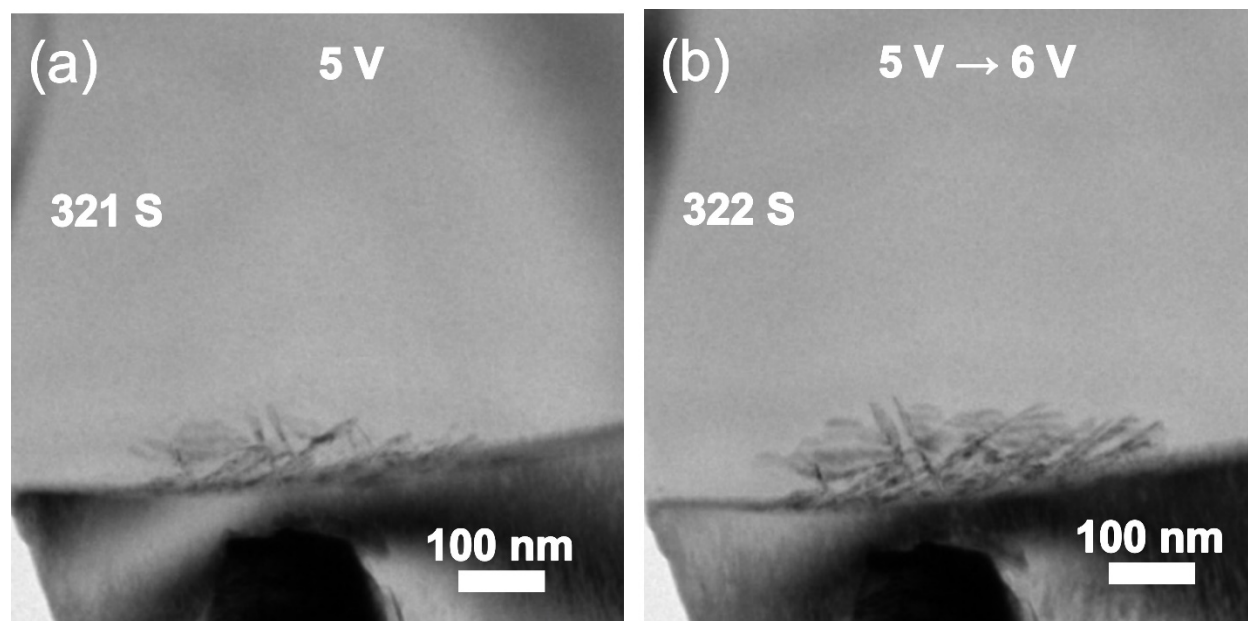


Figure S6. TEM snapshots showing the new filamentary event happened adjacent to previous filaments area when voltage increased from 5V to 6V.